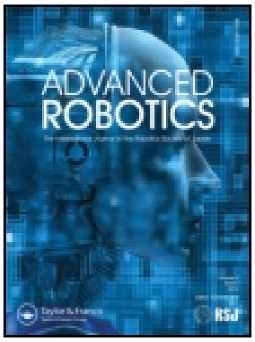

Advanced Robotics

ISSN: 0169-1864 (Print) 1568-5535 (Online) Journal homepage: http://www.tandfonline.com/loi/tadr20

Large attitude change flight of a quad tilt rotor unmanned aerial vehicle

Atsushi Oosedo, Satoko Abiko, Shota Narasaki, Atsushi Kuno, Atsushi Konno & Masaru Uchiyama

ADVANCED ROBOTICS, 2016
VOL. 30, NO. 5, 326–337
http://dx.doi.org/10.1080/01691864.2015.1134344

FULL PAPER

Large attitude change flight of a quad tilt rotor unmanned aerial vehicle

Atsushi Oosedo[a], Satoko Abiko[a], Shota Narasaki[a], Atsushi Kuno[a], Atsushi Konno[b] and Masaru Uchiyama[a]

[a]Department of Mechanical Systems and Design, Graduate School of Engineering, Tohoku University, Sendai, Japan; [b]Division of System Science and Informatics, Hokkaido University, Sapporo, Japan

ABSTRACT
Quadrotor unmanned aerial vehicles (UAVs) have been actively used in various fields. However, only the altitude and the attitude in three degrees of freedom can be independently controlled since quadrotor UAVs are underactuated systems. A quad tilt rotor UAV solves the problem of an underactuated system in a general quadrotor UAV. The quad tilt rotor UAV can control both position and attitude independently by tilting the directions of the propellers. However, the flight control system in a wide range of attitudes has not been discussed yet, for example a UAV can fly and hover with a 90° pitch angle, and it can even flip over when the thrust direction is tilted in a wide enough range. In this paper, we present the attitude transition flight control system for pitch angles ranging from 0° to 90° since flight conditions with a 90° pitch angle significantly differs from that in a conventional quadrotor UAV flight. We construct an adequate control system for a flight with a wide range of attitude conditions.

ARTICLE HISTORY
Received 27 February 2015
Revised 22 July 2015
Accepted 20 November 2015

KEYWORDS
Tilt rotor aircraft; quadrotor; unmanned aerial vehicle; flight control; motion planning

1. Introduction

In recent years, unmanned aerial vehicles (UAVs) have been actively used in various fields. Among the various types of UAVs, quadrotor UAVs are being exploited in the fields of autonomous aerial photography and surveying. The main advantages of these vehicles are that they are low cost, simple, and can be miniaturized. Further, quadrotor UAVs are able to move with exact positioning and hovering capabilities. A quadrotor UAV generally moves with six degrees of freedom (DOF) with only four DOF control inputs, which means that it is an underactuated system.[1,2] Therefore, with this system configuration, only the altitude and attitude in three DOF can be independently controlled, while the translation motion can be achieved by tilting the airframe for generating the horizontal component of propulsion. If quadrotor UAVs had the capability of flying to an arbitrary position and attitude independently, they would complete the above mentioned tasks with higher performance and become even more widespread in various applications (for example, indoor flights where flight space is limited).[3,4]

To solve the above problem, several studies on multirotor UAVs with actuators other than thrusters have been carried out. One solution employs a combination of variable pitch propellers and inclining tilted propeller planes. Kaufman et al. [5] proposed a novel hexarotor UAV concept that is capable of hovering at any attitude. The variable pitch propeller planes of their proposed UAV are fixed to the body such that two propellers exist on each of the three planes, thereby allowing for three-dimensional (3D) force vectors and moment vectors at any attitude. However, there is a problem of energy wastage at an attitude since every propeller plate is fixed at a different tilt angle. Another 6-DOF flight control approach was proposed by Long et al. They developed a novel actuation concept UAV which has a thrust vector system.[6] Their UAV realizes 6-DOF flight control, but the flight orientation is limited by the airframe structure.

Our research focuses on a quadrotor UAV with tilting propellers (rotors). A tilt rotor mechanism can suppress wasteful power consumption since this mechanism can change the direction of thrust with respect to the attitude change. Previous works [7,8] have also discussed a novel concept for a quadrotor UAV with actuated tilting propellers where the propellers are able to rotate around the axes connecting them to the main body frame. Ryll et al. developed a quadrotor UAV with eight control inputs that allow for independent position and attitude control by tilting the propellers themselves instead of changing the attitude of the body. They employed linearized compensation control based on dynamics,[9] and also succeeded in 6-DOF flight experiments; however, the range of the tilting angle was relatively narrow.[10] Segui-Gasco et al. [11,12] developed a UAV with 12 actuators, of

CONTACT Atsushi Oosedo atsushi.oosedo.jp@ieee.org
This paper is selected as the 'Cutting Edge of Robotics in Japan' by the Editorial Committee of Advanced Robotics.

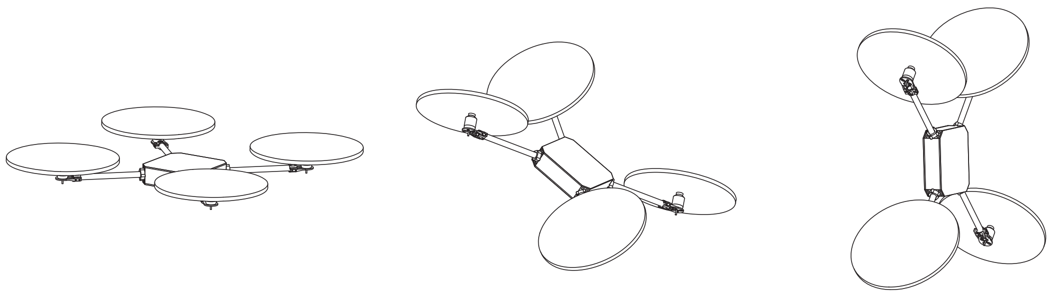

(a) Normal (Conventional) Flight (b) Tilted Flight (c) Perpendicularly-oriented Flight

Figure 1. Independent position and attitude control by a quad tilt rotor UAV.

which four motors were used for propeller rotations and eight servo motors were used for two DOF tilting motion in each propeller. Although the proposed concept could arbitrarily determine the directions of propeller thrust, it required rather complex control calculations, and was difficult to achieve stable flight and led to frequent flight failure. Further, the tilting propeller mechanism also improves the yaw control performance.[13] Elfeky et al. [14] simulated the benefit of tilting propellers on yaw control performance and compared it to a conventional quadrotor UAV.

Although the previous studies could achieve independent position and attitude control, the flight performance in a wide range of attitudes has not been discussed yet, for example the UAV flies and hovers with a 90° pitch angle (Figure 1(c)) and even the UAV can flip over when the range of the tilting motor is wide enough. Such flight conditions allow the UAV to fly more easily in narrow space and make it possible to work on vertical wall surfaces.

In this paper, we discuss the attitude transition flight control system for pitch angles ranging from 0° to 90° (perpendicularly-oriented flight, as shown in Figure 1(c)) since the flight condition at a 90° pitch angle significantly differs from that in a conventional quadrotor UAV. An adequate control system and sufficient experimental validation are necessary for stable flight in a wide range of attitude conditions. This paper presents a quad tilt rotor UAV developed with four tilting mechanisms for four propeller units. We specify the dynamics model of the quad tilt rotor vehicle and describe the flight control systems for different flight conditions. Further, we also discuss a method for switching the control system with respect to the vehicle attitude.

2. Development of a quad tilt rotor UAV

This section discusses the developed quad tilt rotor UAV and its control equipment. The developed UAV has eight control inputs, four of which are used for the rotation of the propeller, and four of which are used for the tilting motion for each propeller.

2.1. Fuselage

Figure 2 shows the developed quad tilt rotor UAV. It weighs 1.4 kg, has a diameter of 0.45 m (without propellers), and a height of 0.10 m. The body frame of the UAV is constructed from a medium density fiberboard (MDF) and each rotor rod is made of carbon fiber.

The tilt rotor mechanism is uniquely developed in our laboratory. The rotor is tilted using of a radio-controlled servo (MD260, Hnege Co), and the rotor rods radiating from the center of the body. The root of the rods is mounted on the rotation axis of the servo. Each rotor rod is supported by a bearing. Hence, the tilting of the rotor is not restricted by the tilt rotor mechanism. The tilting angle has a range of 0° to 260°. Each of the mounts for the servo, rod, and bearing are developed using a 3D printer.

A fixed pitch propeller and a brushless DC motor (D2836/8 1100KV, Turnigy Co) are used as propulsion units. The diameter of the propeller is 0.2794 m and the pitch is 0.11938 m. The motor controllers (Plush 25amp, Turnigy Co) are mounted inside the body and they do not rotate with the propulsion units. The resulting thrust-to-weight ratio is 1.75.

2.2. Electronics

We developed a flight control board for the developed UAV. A commercially available microcomputer (RX62T, Renesas Technology) is used as the main computer, which calculates control inputs using data from each sensor module and sends command signals to each motor. The maximum control outputs are 12 channels. The control frequency is 200 Hz. The developed board is equipped with a 9-DOF inertial measurement unit in a single chip (MPU 9150, InvenSense). Flight logs are recorded on a micro-SD card.

Table 1. Nomenclature.

i	: rotor number ($i = 1 - 4$)
j	: axis ($j = x, y, z$)
$\{\cdot\}_{cur,ref}$	: current and reference parameter
Σ_W	: earth-fixed coordinate system
Σ_B	: body-fixed coordinate system
Σ_{Pi}	: propeller-fixed coordinate system
$\boldsymbol{O}_{W,B,P_i}$	: origin of each coordinate system
m	: mass of the UAV
(u, v, w)	: velocity with respect to Σ_B
(p, q, r)	: angular velocity around each axis of Σ_B
Ω_i	: propeller revolution speed of each rotor
T_i	: thrust force of each motor
Q_i	: torque of each motor
k_T	: thrust constant
k_Q	: torque constant
$I_{B_{jj}}$	: principal moment of inertia of the UAV including rotors
$I_{P_{jj}}$	: principal moment of inertia of the rotor
${}^B\boldsymbol{R}_A$	: rotation matrix from A to B
$\boldsymbol{R}_{ref}$	: rotation matrix of the reference attitude w.r.t Σ_W
$\boldsymbol{R}_{cur}$	: rotation matrix of the current attitude w.r.t Σ_W
η	: angle of rotation between Σ_B and $\Sigma_{B'}$
ω_j	: attitude error of each axis of Σ_B
δ_j	: attitude control value
C_1	: conversion constant from the torque to the tilt angle
C_2	: conversion constant from the force to the tilt angle
$\boldsymbol{P}_W$	: position of the UAV w.r.t Σ_W
$e_{W,B}$	: position of error
F_{Wj}	: force of each axis component in Σ_W

The position is obtained from a global positioning system (GPS) receiver module (LEA-6H module, uBlox) in outside flight and the refresh rate of GPS is 5 Hz. On the other hand, current position is obtained from a motion capture system in indoor flight. The refresh rate of the motion capturer system is 200 Hz, and the current position are send to the UAV from the processing computer by the ZigBee module.

3. Dynamics modeling

This section explains the coordinate systems and the dynamics model of the quad tilt rotor UAV. The symbols used in this section are listed in Table 1.

3.1. Coordinate systems

Figure 3 shows the coordinate systems defined in this paper. The term Σ_W defines the earth-fixed coordinate system (inertial coordinates), Σ_B defines the body-fixed coordinate system, and Σ_{P_i} ($i = 1 - 4$) defines the rotor-fixed coordinate system. The earth-fixed coordinate system defines the X_W axis as true north, the Y_W axis as east, and the Z_W axis as being perpendicular and pointing downward.

The rotation motion about the X_B, Y_B, and Z_B axes are defined as roll, pitch, and yaw and the rotation angle around each axis is denoted as ϕ, θ, and ψ, respectively. The coordinate system of the aircraft is consistent in every

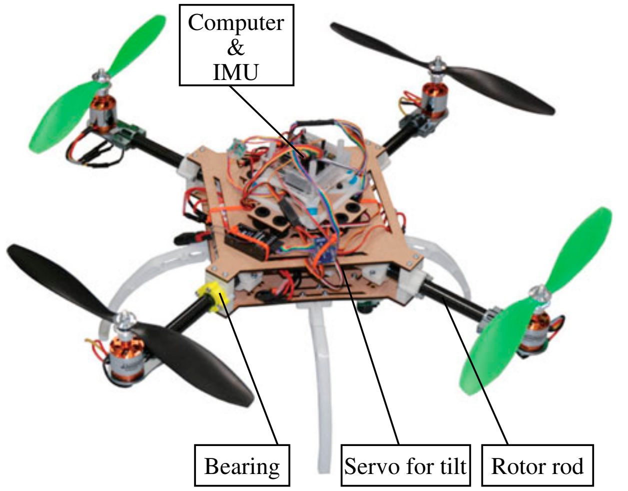

Figure 2. The developed quad tilt rotor UAV.

flight modes. The direction from the motor to the center of gravity (COG) is rotated by 45° around the Z_B axis with respect to Σ_B. Further, X_{P_i} is defined as the tilting actuation axis and Z_{P_i} is defined as the negative direction on the thrust axis. The ith actuated tilting angle is defined as α_i.

Moreover, the auxiliary coordinate system $\Sigma_{B'}$ is also defined. $\Sigma_{B'}$ is rotated by 45° around the Z_B axis so that the $X_{B'}$ axis coincides with the direction from O_{P_3} to O_{P_1} and the $Y_{B'}$ axis coincides with the direction from O_{P_4} to O_{P_2}. The auxiliary coordinate system $\Sigma_{B'}$ is used for calculation of the offset tilt angle in Section 4.3.

3.2. Dynamics modeling

The equations of motion of the quad tilt rotor UAV are discussed in this section. In the given equations, the term s_i and c_i are expressed as $s_i = \sin(\alpha_i)$ and $c_i = \cos(\alpha_i)$, respectively. The translational and rotational dynamic equations of the mathematical model in the aircraft body coordinates are expressed as follows:

- Translational dynamic equations

$$m\left(\dot{u} - rv + qw\right) = \sin\eta(-T_1s_1 - T_2s_2 + T_3s_3 + T_4s_4) - mg\sin(\theta). \quad (1)$$

$$m\left(\dot{v} - pw + ru\right) = \sin\eta(T_1s_1 - T_2s_2 - T_3s_3 + T_4s_4) + mg\sin(\phi)\cos(\theta). \quad (2)$$

$$m\left(\dot{w} - qu + pv\right) = -\sum_{i=1}^{4} T_ic_i + mg\cos(\phi)\cos(\theta). \quad (3)$$

- Rotational dynamic equations

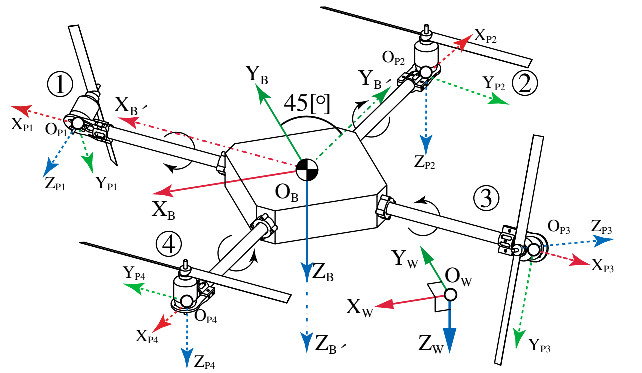

Figure 3. Coordinate systems.

$$
\begin{aligned}
I_{B_{xx}}\dot{p} = {} & (I_{B_{yy}} - I_{B_{zz}})qr + l\cos\eta(-T_1c_1 - T_2c_2 \\
& + T_3c_3 + T_4c_4) \\
& + \cos\eta(Q_1s_1 - Q_2s_2 - Q_3s_3 + Q_4s_4) \\
& + \cos\eta(I_{P_{xx}}\ddot{\alpha}_1 - I_{P_{xx}}\ddot{\alpha}_3) \\
& + \sin\eta(I_{P_{xx}}\ddot{\alpha}_2 - I_{P_{xx}}\ddot{\alpha}_4) \\
& + I_{P_{xx}}\sin\eta\left(q\sum_{i=1}^{4}(-1)^{i-1}\Omega_i c_i + r(\Omega_1 s_1\right. \\
& \left. - \Omega_3 s_3)\right) - I_{P_{xx}}\sin\eta(\dot{\alpha}_2\Omega_2c_2 - \dot{\alpha}_4\Omega_4c_4). \qquad (4)
\end{aligned}
$$

$$
\begin{aligned}
I_{B_{yy}}\dot{q} = {} & (I_{B_{zz}} - I_{B_{xx}})pr + l\cos\eta(T_1c_1 - T_2c_2 \\
& - T_3c_3 + T_4c_4) \\
& + \cos\eta(-Q_1s_1 - Q_2s_2 + Q_3s_3 + Q_4s_4) \\
& + \sin\eta(I_{P_{xx}}\ddot{\alpha}_1 - I_{P_{xx}}\ddot{\alpha}_3) + \cos\eta(I_{P_{xx}}\ddot{\alpha}_2 - I_{P_{xx}}\ddot{\alpha}_4) \\
& - I_{P_{xx}}\sin\eta\left(p\sum_{i=1}^{4}(-1)^{i-1}\Omega_i c_i - r(-\Omega_2 s_2\right. \\
& \left. + \Omega_4 s_4)\right) - I_{P_{xx}}\sin\eta(\dot{\alpha}_1\Omega_1c_1 - \dot{\alpha}_3\Omega_3c_3). \qquad (5)
\end{aligned}
$$

$$
\begin{aligned}
I_{B_{zz}}\dot{r} = {} & (I_{B_{xx}} - I_{B_{yy}})pq + \sum_{i=1}^{4}\left(T_is_i + (-1)^{i-1}Q_ic_i\right) \\
& + I_{P_{xx}}\left(-p(\Omega_1s_1 + \Omega_3s_3) + q(\Omega_2s_2 - \Omega_4s_4)\right) \\
& - I_{P_{xx}}\left(\sum_{i=1}^{4}(-1)^{i-1}\alpha_i\Omega_is_i\right). \qquad (6)
\end{aligned}
$$

The thrust and torque generated by a propeller are changed as a function of airflow velocity into a propeller. However, assuming that the flight condition is extremely close to the state of hovering, the airflow velocity becomes 0 [m/s]. Hence, the change of airflow velocity is ignored in this study. The thrust and torque can then defined as follows:

$$T_i \fallingdotseq k_T\Omega_i^2, \qquad (7)$$

$$Q_i \fallingdotseq k_Q\Omega_i^2. \qquad (8)$$

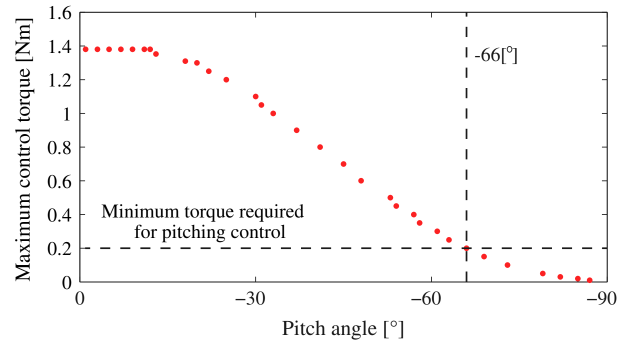

Figure 4. Maximum pitch control torque.

4. Flight control system

This section describes the flight control systems for different flight conditions and discusses methods for switching control systems with respect to the attitude of the UAV.

4.1. Concept of control design

A remarkable capability of the quad tilt rotor UAV is that it can hover at a wide range of attitudes by tilting its propeller units directly. Further, it can move in any direction without changing the attitude of the airframe itself. To achieve 6-DOF flight control, we determine the 'offset tilt angle' in the control design. For example, when the pitch angle of the UAV is controlled to 0°, the offset tilt angle of Σ_{P_1} is determined as 0°; meanwhile, when the pitch angle of the UAV is driven to 90°, the offset tilt angle of Σ_{P_1} is determined as 90°. The detailed calculation of the offset tilt angle is explained in Section 4.3.

On the other hand, the change of the offset tilt angle leads to a decrease of attitude control torque that is generated by the thrust difference of the propellers. Figure 4 shows the calculated maximum pitch control torque generated by the thrust difference between the rotors on Σ_{P_1} and Σ_{P_4} and the rotors on Σ_{P_2} and Σ_{P_3}. As shown in Figure 4, the maximum control torque decreases as the pitch of the UAV decreases. The developed UAV requires a minimum of 0.2 Nm control torque for achieving stable flight. As a result, if the pitch angle is less than −66°, the pitch of the UAV cannot be controlled in stable manner. This pitch angle is obtained from flight simulation. The simulation result shows that when the pitch angle becomes smaller than −66°, the attitude controllability with thrust difference becomes unstable due to the control frequency and the change of the moment of inertia with respect to the inertial coordinates. The control frequency and the moment of inertia depend on the aircraft specific, and the moment of inertia also changes due to the aircraft configuration.

Therefore, we designed two control systems with respect to the attitude of the UAV and they are switched by

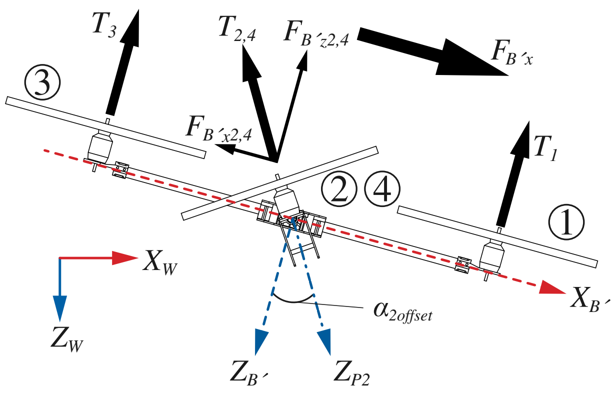

Figure 5. Offset tilt angle.

an attitude change. In this paper, when the pitch angle is between 0 and $-66°$ the flight is defined as being in the normal condition; and when the pitch angle is between -66 and $-90°$ the flight is defined as being in the perpendicular condition. Table 2 lists the thrusts and torques used for translational and rotational motion in the two flight conditions. These control systems realize independent position and attitude control in both flight conditions.

4.2. Control system

Figure 6 shows a block diagram of the flight controller. The flight control system is designed based on a PID controller.

First, the flight plan and the reference parameters are installed in the block labeled as 'Flight Planner'. After the UAV receives a command from an operator, the planner generates the reference attitude and altitude from the prearranged flight plan and current sensor information including the attitude and position. The rotation matrices $\boldsymbol{R}_{ref}$ and $\boldsymbol{R}_{cur}$ are sent to the block labeled as 'Attitude Transition Strategy'. This block calculates the errors around the X_B, Y_B, and Z_B axes of the aircraft body coordinates. In this paper, 'Resolved Tilt-Twist Angle Feedback Control' [15] is used to calculate the attitude error for a high-mobility aircraft. This method increases the stability against large attitude disturbances. These errors, which are defined as ω_j $(j = x, y, z)$, are sent to the block labeled as 'Attitude Controller', where ω_x, ω_y, and ω_z denote the minimum attitude error between the reference and current attitudes around the X_B, Y_B, and Z_B axes, respectively. The PID controller generates control values for attitude control, which are expressed as follows:

$$\delta_j = \left(K_{P_A}\omega_j + K_{I_A}\int \omega_j \mathrm{d}t + K_{D_A}\dot{\omega}_j\right) \quad (j = x, y, z), \tag{9}$$

where K_{P_A}, K_{I_A}, and K_{D_A} are the attitude PID control gains which are determined by the ultimate sensitivity method and tuned via trial and error.

The block labeled 'Position Controller' calculates the position error in the earth-fixed coordinate system. These errors are then translated to the position error in the body-fixed coordinate system in this block. The position controller generates the desired control forces $\boldsymbol{F_B}$. These desired quantities are expressed as follows:

$$\boldsymbol{e}_W = \boldsymbol{P}_{cur} - \boldsymbol{P}_{ref}, \tag{10}$$

$$\boldsymbol{e}_B = ({}^W\boldsymbol{R}_B)^T \boldsymbol{e}_W, \tag{11}$$

$$\begin{bmatrix} F_{B_x} \\ F_{B_y} \\ F_{B_z} \end{bmatrix} = K_{P_B}\boldsymbol{e_B} + K_{I_B}\int \boldsymbol{e_B}\mathrm{d}t + K_{D_B}\dot{\boldsymbol{e}}_{\boldsymbol{B}} + ({}^W\boldsymbol{R}_B)^T \begin{bmatrix} 0 \\ 0 \\ mg \end{bmatrix}, \tag{12}$$

where corresponds to the total thrust, K_{P_B}, K_{I_B}, and K_{D_B} represent the position PID control gains. These control torques and forces are sent to the block labeled 'Distributor', which determines the reference tilt angle and the propeller revolution speed of each motor. The calculation of the distribution is presented in Section 4.4.

4.3. Calculation of offset tilt angle

Figure 5 shows the concept used for the calculation of the offset tilt angle. This angle is necessary for stationary hovering with a constant attitude of the UAV.

First, $\boldsymbol{F_W}$ is estimated from the current tilt angle and thrust. Second, in order to simplify the calculation, $\boldsymbol{F_W}$ is converted to $\boldsymbol{F_{B'}}$. Third, each offset tilt angle to cancel $F_{B'_{x,y}}$ is calculated. The horizontal component of the thrust produced by $\alpha_{1_{offset}}$ and $\alpha_{3_{offset}}$ cancels out $F_{B'_y}$ and that of thrust produced by $\alpha_{2_{offset}}$ and $\alpha_{4_{offset}}$ cancels out $F_{B'_x}$. These offset tilt angles are expressed as follows:

$$\alpha_{1_{offset}} = -\sin^{-1}\left(\frac{F_{B'_y} - F_{B'_{y3}}}{T_1}\right), \tag{13}$$

$$\alpha_{2_{offset}} = \sin^{-1}\left(\frac{F_{B'_x} - F_{B'_{x4}}}{T_2}\right), \tag{14}$$

$$\alpha_{3_{offset}} = \sin^{-1}\left(\frac{F_{B'_y} - F_{B'_{y1}}}{T_3}\right), \tag{15}$$

$$\alpha_{4_{offset}} = -\sin^{-1}\left(\frac{F_{B'_x} - F_{B'_{x2}}}{T_4}\right), \tag{16}$$

Table 2. Control force and torque.

			Normal condition		Perpendicular condition
Translation	X_W	:	Horizontal component of thrust by the tilt of rotors	:	Horizontal component of thrust by tilt of all rotors
	Y_W	:	Horizontal component of thrust by the tilt of rotors	:	Differential thrust between rotors (1&3) and (2&4)
	Z_W	:	Total thrust	:	Total thrust
Rotation	X_B	:	Differential thrust between rotors (1&2) and (3&4)	:	Generated torque by the tilting rotor between rotors (1&2) and (3&4)
	Y_B	:	Differential thrust between rotors (1&4) and (2&3)	:	Generated torque by tilting rotor between rotors (1&4) and (2&3)
	Z_B	:	Tilt of all rotors	:	Differential thrust between rotors (1&2) and (3&4)

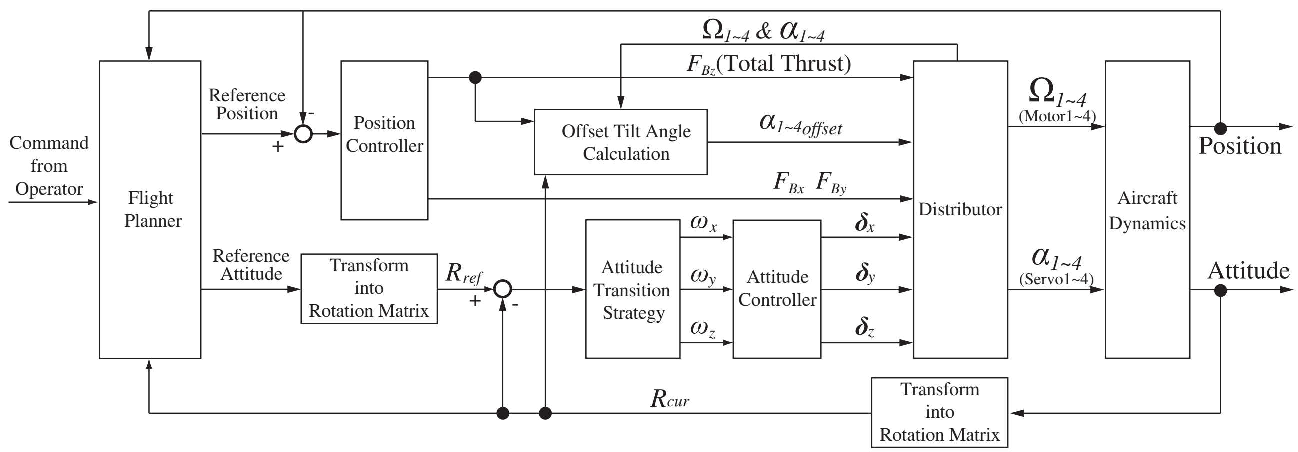

Figure 6. Block diagram of control system.

where $F_{B'_{ji}}$ is the force of the j axis component of $\Sigma_{B'}$ produced by the i-th propeller. These offset tilt angles are sent to the distributor.

4.4. Distribution of the control parameters and switching methods of the control systems

The distributor determines the reference tilt angle and the propeller revolution speed of each motor based on Table 2. The reference propeller revolution speed and tilt angle of the rotors in the two conditions are expressed as follows:

- Normal condition

$$\Omega_{1_{norm}} = \sqrt{\frac{F_{Bz}}{4k_T} + \frac{\delta_x}{4k_Q} - \frac{\delta_y}{4k_Q}}, \tag{17}$$

$$\Omega_{2_{norm}} = \sqrt{\frac{F_{Bz}}{4k_T} + \frac{\delta_x}{4k_Q} + \frac{\delta_y}{4k_Q}}, \tag{18}$$

$$\Omega_{3_{norm}} = \sqrt{\frac{F_{Bz}}{4k_T} - \frac{\delta_x}{4k_Q} + \frac{\delta_y}{4k_Q}}, \tag{19}$$

$$\Omega_{4_{norm}} = \sqrt{\frac{F_{Bz}}{4k_T} - \frac{\delta_x}{4k_Q} - \frac{\delta_y}{4k_Q}}. \tag{20}$$

$$\alpha_{1_{norm}} = \alpha_{1_{offset}} - C_1\delta_z/4 - C_2F_{Bx}/4 + C_2F_{By}/4, \tag{21}$$

$$\alpha_{2_{norm}} = \alpha_{2_{offset}} - C_1\delta_z/4 - C_2F_{Bx}/4 - C_2F_{By}/4, \tag{22}$$

$$\alpha_{3_{norm}} = \alpha_{3_{offset}} - C_1\delta_z/4 + C_2F_{Bx}/4 - C_2F_{By}/4, \tag{23}$$

$$\alpha_{4_{norm}} = \alpha_{4_{offset}} - C_1\delta_z/4 + C_2F_{Bx}/4 + C_2F_{By}/4. \tag{24}$$

- Perpendicular condition

$$\Omega_{1_{perp}} = \sqrt{\frac{F_{Bz}}{4k_T} + \frac{F_{By}}{4k_T} - \frac{\delta_z}{4k_Q}}, \tag{25}$$

$$\Omega_{2_{perp}} = \sqrt{\frac{F_{Bz}}{4k_T} - \frac{F_{By}}{4k_T} - \frac{\delta_z}{4k_Q}}, \tag{26}$$

$$\Omega_{3_{perp}} = \sqrt{\frac{F_{Bz}}{4k_T} + \frac{F_{By}}{4k_T} + \frac{\delta_z}{4k_Q}}, \tag{27}$$

$$\Omega_{4_{perp}} = \sqrt{\frac{F_{Bz}}{4k_T} - \frac{F_{By}}{4k_T} + \frac{\delta_z}{4k_Q}}. \tag{28}$$

$$\alpha_{1_{perp}} = \alpha_{1_{offset}} - C_2F_{Bx}/4 - C_1\delta_x/4 + C_1\delta_y/4, \tag{29}$$

$$\alpha_{2_{perp}} = \alpha_{2_{offset}} - C_2F_{Bx}/4 - C_1\delta_x/4 - C_1\delta_y/4, \tag{30}$$

$$\alpha_{3_{perp}} = \alpha_{3_{offset}} + C_2F_{Bx}/4 - C_1\delta_x/4 + C_1\delta_y/4, \tag{31}$$

$$\alpha_{4_{perp}} = \alpha_{4_{offset}} + C_2F_{Bx}/4 - C_1\delta_x/4 - C_1\delta_y/4. \tag{32}$$

where two subscripts $\{\cdot\}_{i_{norm}}$ and $\{\cdot\}_{i_{perp}}$ express the normal and perpendicular conditions, respectively.

Moreover, the switching method of these control systems is implemented in the distributor block. When the attitude is drastically changed, the switching of the control systems in the two flight conditions becomes significant. This paper proposes two switching methods for flight control.

The first switching method is the simplest way that the two control systems in two flight conditions are simply switched at $\theta = -66°$. When the θ is $-66°$ or larger, the UAV is controlled by the control system of the normal condition. If the θ is under the $-66°$, the UAV is controlled by the control system of the perpendicular condition. Therefore, when the reference θ is $-66°$ with the first switching method, a chattering may be caused. To avoid a chattering, the reference θ is obtained without depending on the current attitude during the transition flight

The second switching method is superimposition of two control systems with trigonometric functions, whose augment is the pitch angle. In this method, the propeller revolution speed and the tilt angle during the transition are calculated as follows:

$$\Omega_i = \sqrt{\frac{F_{Bz}}{4k_T} + \left(\Omega_{i_{norm}}^2 - \frac{F_{Bz}}{4k_T}\right)\cos\theta - \left(\Omega_{i_{perp}}^2 - \frac{F_{Bz}}{4k_T}\right)\sin\theta}, \tag{33}$$

$$\alpha_i = \alpha_{i_{offset}} + (\alpha_{i_{norm}} - \alpha_{i_{offset}})\cos\theta - (\alpha_{i_{perp}} - \alpha_{i_{offset}})\sin\theta. \tag{34}$$

5. Verification

The designed systems for independent position and attitude control are validated by both simulations and experiments. Firstly, to verify the proposed switching methods for a transition flight, a transition flight simulation is performed. Next, three kinds of experiments are conducted: (i) the normal condition, (ii) the perpendicular condition, and (iii) the transition from the normal condition to the perpendicular condition. In the verification of the transition, the pitch of the UAV is continuously changed from 0 to $-90°$.

When $\theta = -90°$, the attitude cannot be represented by roll, pitch, and yaw angles (ZYX Euler angles) due to the mathematical singularity. Therefore, the ZXY Euler angle expressions are used in the attitude controller. The ZXY Euler angles are defined as σz, σx and σy, respectively. For example, σy denotes the attitude of the Y_B axis.

5.1. Simulation verification

This subsection presents two transition flight simulations. In these simulations we carried out the case of transition from the normal condition to the perpendicular condition. A 3D flight simulator is developed using the technical computing language MATLAB R2012a (MathWorks, Inc.). The simulator requires model parameters in advance. Among the model parameters, the moment of inertia is obtained from a precise 3D CAD model developed with 3D CAD software (Solidworks 2012). Hence, we assume that the moment of inertia of the simulation model is approximately identical to the physical parameters. The mass and the delay time of the actuators response are simply measured by the measurement experiment.

Flight control systems for the normal condition, the perpendicular condition, and the two switching methods are implemented in the simulator. In the simulation, the reference σy decreases from 0° to $-90°$ in 2 s. The reference σx and σz is 0, and the reference position is 0 m.

Figures 7 and 8 show the sequential snapshots of simulations for two switching methods. The figures show that the large attitude change is achieved in both methods. Moreover, the position of two simulations keeps almost the initial position during the transition.

Figures 9(a)–10(c) show the attitude, position and tilt angle in each switching method. From Figures 9(a) and 10(a), it can be observed that the attitude response of the second switching method is faster than that of the first switching method because of the compensation of the control torque with superimposition of two control systems, although the convergence to the desired attitude is not tuned enough even in the second switching method. In the first switching method, two control systems are simply switched at the time when the aircraft reached to $\sigma y = -66°$, $t = 1.35$ s. Hence, until $t = 1.35$ s, the attitude control torque is generated according to the performance limitation as shown in Figure 4. After that, the control system is switched to the perpendicular condition, therefore, the aircraft can produce larger attitude control torque to decrease the attitude error. On the other hand, the second switching method uses a superimposition of two control systems followed by Equations (33) and (34). Therefore, during the transition, even in pitch angle smaller than $\sigma y = -66$ [°], the aircraft can generate enough attitude control torque. Besides, no chattering on the attitude profile is observed at the time when the aircraft reached to $\sigma y = -66°$ at $t = 0.81$ s. Since the compensation improved the attitude control performance by about $\sigma y = -66°$, the attitude error decreases and the response accelerates. Moreover, Figures 9(b) and 10(b) show that the improvement of the attitude control performance reduce the position error.

Figure 9(c) shows that the tilt angle is changed rapidly at $\sigma y = -66°$. This rapid change of the tilt angle occurs

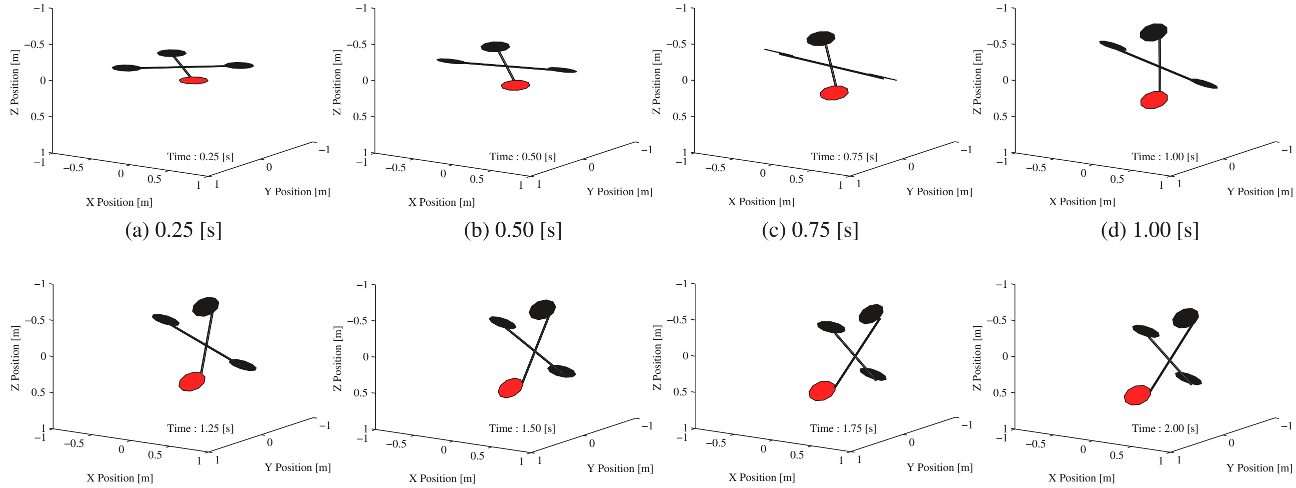

(a) 0.25 [s] (b) 0.50 [s] (c) 0.75 [s] (d) 1.00 [s]

(e) 1.25 [s] (f) 1.50 [s] (g) 1.75 [s] (d) 2.00 [s]

Figure 7. Snapshots of the transition simulation with the first switching method.

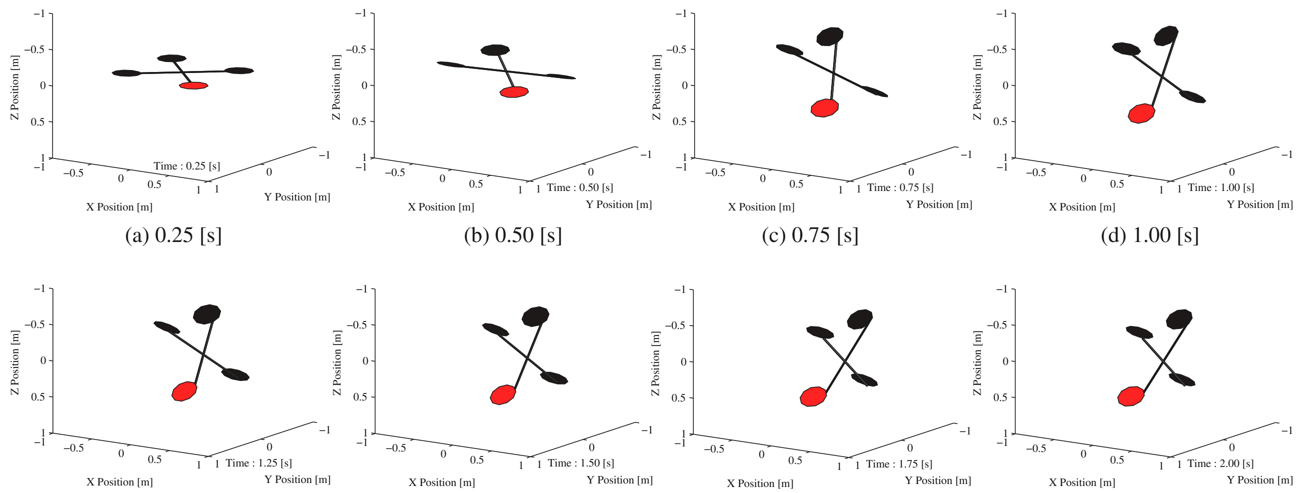

(a) 0.25 [s] (b) 0.50 [s] (c) 0.75 [s] (d) 1.00 [s]

(e) 1.25 [s] (f) 1.50 [s] (g) 1.75 [s] (d) 2.00 [s]

Figure 8. Snapshots of the transition simulation with the second switching method.

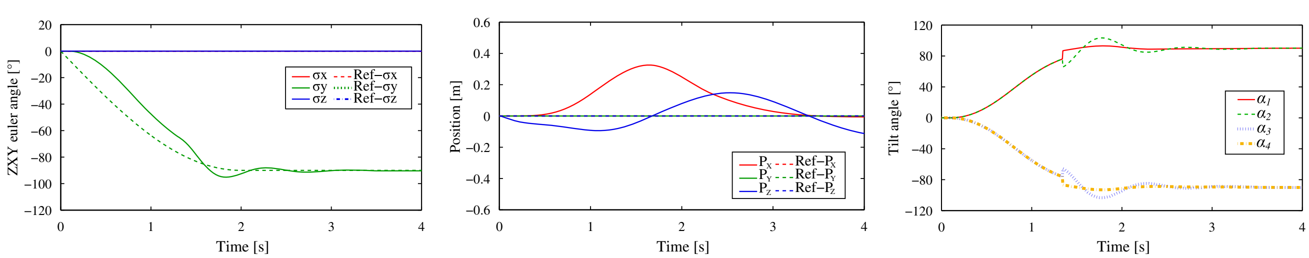

(a) Attitude (b) Position (c) Tilt angle

Figure 9. Simulation results of the first switching method.

since the control system is simply switched from the normal condition to the perpendicular condition at $\sigma y = -66°$. In contrast, Figure 10(c) shows that the tilt angle in the second switching method changed smoothly.

These simulation results show that the designed independent control systems of position and attitude succeeded in 6-DOF flight control with two significantly different flight conditions. The compensation of control torque provides stabilization of the flight control.

5.2. Experimental verification

The normal condition, the transition and the perpendicular condition flight control experiments are conducted

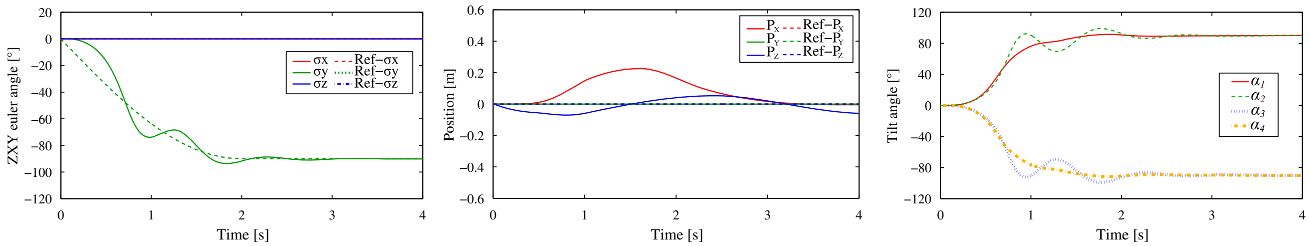

(a) Attitude (b) Position (c) Tilt angle

Figure 10. Simulation results of the second switching method.

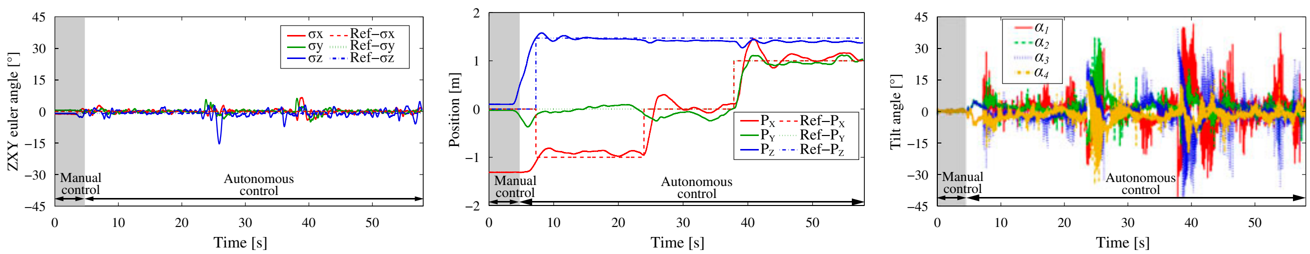

(a) Attitude (b) Position (c) Tilt angle

Figure 11. Experiment results of the normal condition flight.

indoors, and the position is measured by motion capture systems. The reference attitude and position are implemented in the 'Flight Planner' block in Figure 6. The UAV flies according to the installed flight plan.

5.2.1. Normal condition

The experimental results of the normal condition flight experiment are shown in Figure 11(a)–(c).

Figure 11(a) and (b) shows the attitude and position of the UAV. Note that the reference attitude is $(\sigma z, \sigma x, \sigma y) = (0, 0, 0)$ [°] throughout the experiment. The position of the UAV follows the reference with constant attitude. However, when the reference position is changed at $t = 7.64$, 23.80, and 30.87 s, the attitude is disturbed. The maximum error of σx and σy are $\pm 5°$ and that of σz is -15o. The disturbance to the attitude is caused by the reaction torque of the tilting rotor. Figure 11(c) shows the tilt angle of each motor. When the reference position changes, the tilt servos rotate quickly and large rotation because the reference position is given as a step input. Hence, the UAV receives the reaction torque of each tilting motor. In this research, the compensator of the reaction torque which is generated by the tilting motor is not implemented. Therefore, the attitude is influenced by the tilt reaction torque when the rotor rotates quickly. However, the attitude rapidly converges to the reference after the occurrence of the disorder. As a result, the designed control system succeeded in a 6-DOF flight control within the normal orientation condition. The disturbance of the attitude might be reduced by the compensating the tilt reaction torque or limiting the tilt rotation speed.

5.2.2. Transition from the normal condition to the perpendicular condition

The designed 6-DOF flight control system for the two flight conditions and the second switching method were implemented on the developed UAV, and then an indoor flight experiment was conducted. The UAV controls its attitude and position autonomously. After the UAV receives a start command for transition from an operator, the UAV commences an autonomous transition from the normal condition to the perpendicular condition.

Figure 12 shows snapshots of the transition flight experiment from the normal condition to the perpendicular condition. The transition flight starts at $t = 11.85$ s and ends $t = 12.65$ s. Although the attitude of the UAV changes rapidly, it is controlled in a stable manner during the experiment. Moreover, the UAV maintains a constant altitude across the transition phase.

Figure 13(a)–(c) shows the attitude, position and tilt angle during the experiment.

Figure 13 shows that σy transits from 0 to $-90°$ in 0.8 s. This term decreases faster during the experiment than during the simulation since the reference pitch angle is given as a step input. Therefore, there is an overshoot of about $+11°$. After the transition, there are no large attitude errors during the flight. Figure 13(b) shows that the position of the vehicle follows the reference during the transition. Figure 13(c) shows that the tilt angle changes with respect to the attitude error and the position error. When σy overshoots $\sigma y = -90°$, each rotor tilts to reduce the error of σy. The tilt angle changes smoothly

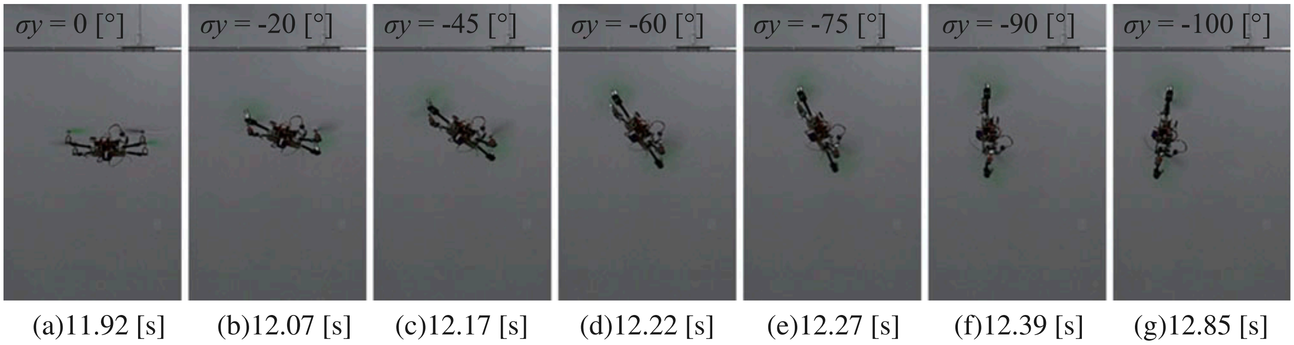

Figure 12. Snapshots of the transition to the perpendicular condition.

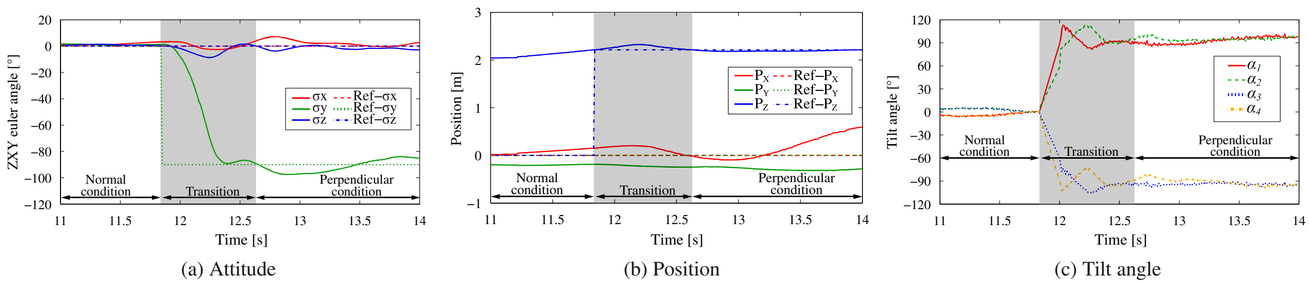

Figure 13. Experiment results of the transition flight.

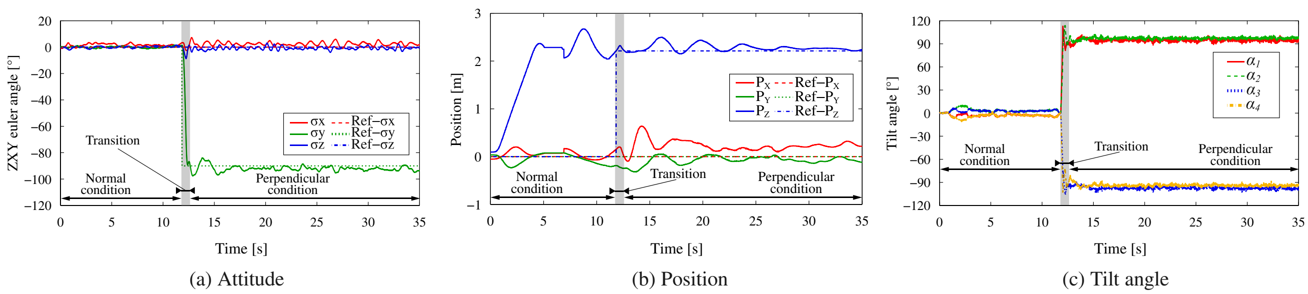

Figure 14. Experiment results of the perpendicular flight.

around $\sigma y = -66°$ because the switching method switched two control systems in an efficient way.

This experimental result shows that the designed control systems succeeded in 6-DOF flight control with two significantly different flight conditions. The flight experiment verifies the effectiveness of the transition procedure for achieving such conditions.

5.2.3. Perpendicular condition

The experimental results of the perpendicular condition flight experiment are shown in Figure 14(a)–(c).

Figure 14(a) and (b) shows the attitude and position of the UAV. Note that the reference attitude in the perpendicular condition is $(\sigma z, \sigma x, \sigma y) = (0, 0, -90)°$. The second switching method is implemented in this test. A disturbance to attitude and position are observed just after the transition; however, the UAV eventually follows the reference position in a perpendicular orientation after the transition. The maximum position error is 0.5 m on the X_W axis, and the maximum attitude error of σy are $\pm 10°$. It is clear from Figure 14(c) that in order to reduce these errors, tilt motors rotate large rotation right after the transition. The variation quantity of the tilt angles reduces with the decrease in these errors. As a result, the designed control system succeeded in 6-DOF flight control within the perpendicular orientation condition.

6. Conclusions

This paper presented the development of a quad tilt rotor UAV and the verification of the designed independent control systems for a wide range of attitude conditions. We developed a quad tilt rotor UAV which has eight control inputs of which four inputs control propeller revolutions and the remaining four inputs tilt the directions. The developed UAV has a wide range tilting angle range of 0 to $+260°$. Therefore, we designed control systems for significantly different attitude conditions such as normal and perpendicular conditions. Furthermore, we proposed two switching methods for the flight control systems with respect to the attitude of the UAV. These control systems and switching methods were implemented on the developed UAV, and verification experiments were performed. The experimental results showed that the control systems succeeded in full autonomous 6-DOF flight control with two significantly different conditions and during the transition between these conditions. The flight experiments verified the effectiveness of the transition procedure.

In the future, we aim to implement compensation of the reaction torque that is generated by the tilting motor. Moreover, we will challenge the missions considering features of a quad tilt rotor UAV such as wall surface investigation.

Disclosure statement

No potential conflict of interest was reported by the authors.

Funding

This work was supported by Grant-in-Aid for Japan society for the promotion of science fellows [grant number 25-4220].

Notes on contributors

Atsushi Oosedo received the BE from Tokai University, Kanagawa, Japan, in 2009, in the Aeronautics and Astronautics, and the ME and PhD degree from Tohoku University, Sendai, Japan, in 2011, and 2014 in Aerospace Engineering. He became a research fellowship for Young Scientists in the Japan Society for the Promotion of Science from 2013 to 2014. Since 2015, he is a researcher of Aeronautical Technology Directorate, Japan Aerospace Exploration Agency. His major fields of interest include design and control of unmanned aerial vehicles and associated equipment.

Satoko Abiko received BE and MS degrees in aerospace engineering from Tohoku University, Japan in 2000 and 2002, respectively. She received Dr Eng degree from Tohoku University, Japan in 2005. From 2003 to 2005, she was a research fellow of the Japan Society for the Promotion of Science. She was a visiting scientist in Institute of Robotics and Mechatronics, German Aerospace Center (DLR) from 2005 to 2009. From 2009 to 2015, she was an assistant professor of the Department of Mechanical Systems and Design in Tohoku University, Japan. Since 2015, she has been with the School of Engineering, Shibaura Institute of Technology, Japan and currently is an Associate Professor of the Department of Electrical Engineering. Her research interests cover dynamics and control of space robotic systems including free-flying space robots and flexible manipulator systems, unmanned aerial vehicles and their applications.

Shota Narasaki received BE degree from Tohoku University, Sendai, Japan in 2013, in Mechanical and Aerospace Engineering. He received MS degree in Mechanical Systems and Design from Tohoku University, 2015. He currently works at Mitsubishi Hitachi Power Systems Co., Ltd.

Atsushi Kuno received BE degree from Tohoku University, Sendai, Japan in 2013, in Mechanical and Aerospace Engineering. He received MS degree in Mechanical Systems and Design from Tohoku University, 2015. He currently works at Isuzu Motors Co., Ltd.

Atsushi Konno received the BE, ME, and PhD degrees in Precision Engineering from Tohoku University, Sendai, Japan, in 1988, 1990, and 1993, respectively. He became a research associate with Tohoku University in 1993, a research associate with the University of Tokyo in 1995, and an associate professor with Tohoku University in 1998. In 2012, he was a professor with Hokkaido University, Sapporo, Japan. His research interests include humanoid robots, unmanned aerial vehicles, surgery simulator, and their applications.

Masaru Uchiyama received BE, ME, and PhD degrees from the University of Tokyo, Tokyo, Japan, in 1972, 1974, and 1977, respectively, all in Mechanical Engineering for Production. Since 1977 to 2015, he had been with the School of Engineering, Tohoku University, Sendai, Japan, and currently is a professor emeritus there. His current research interest is design of intelligent mechanical systems. He is a fellow and an Honorary Member of the Japan Society of Mechanical Engineers, a fellow and an Honorary Member of the Society of Instrument and Control Engineers, a fellow of the Robotics Society of Japan, and a life fellow of IEEE.

References

[1] Castillo P, Lozano R, Dzul AE. Modelling and control of mini-flying machines. Vol. XVI, Advances in industrial control. London: Springer; 2004.

[2] Bouabdallah S, Murrieri P, Siegwart R. Towards autonomous indoor micro VTOL. Auton. Robots. 2005;18:171–183.

[3] Michael N, Shen S, Mohta K, et al. Collaborative mapping of an earthquake-damaged building via groud and aerial robots. J. Field Rob. 2012;29:832–841.

[4] Metni N, Tarek H. A UAV for bridge inspection: visual servoing control law with orientation limits. Autom. Constr. 2007;17:3–10.

[5] Kaufman E, Caldwell K, Lee D, et al. Design and development of a free-floating Hexrotor UAV for 6-DOF Maneuvers. In: Proceedings of the IEEE aerospace conference; 2014 Mar 1–8; Big Sky (MT); 2014. p. 1–10.

[6] Longa Y, Wangb L, Cappelleria DJ. Modeling and global trajectory tracking control for an over-actuated MAV. Adv. Robot. 2014;28:145–155.

[7] Ryll M, Bulthoff HH, Giordano PR. Modeling and control of a quadrotor UAV with tilting propeller. In: Proceedings of the 2012 IEEE international conference on robotics and automation; 2012 May 14–18; St Paul (MN); 2012. p. 4606–4613.

[8] Falconi R, Melchiorri C. Dynamic model and control of an over-actuated quadrotor UAV. Robot Control. 2012;10:192–197.

[9] Ryll M, Bulthoff HH, Giordano PR. First flight tests for a quadrotor UAV with tilting propeller. In: Proceedings of the 2013 IEEE international conference on robotics and automation; 2013 May 6–10; Karlsruhe; 2013. p. 295–302.

[10] Ryll M, Bulthoff HH, Giordano PR. A novel overactuated quadrotor unmanned aerial vehicle: modeling, control, and experimental validation. IEEE Trans. Control Syst. Technol. 2014; p. 1–17.

[11] Segui-Gasco P, Al-Rihani Y, Shin HS, et al. A novel actuation concept for a multi rotor UAV. In: Proceedings of the international conference on unmanned aircraft systems; 2013 May 28–31; Atlanta (GA); 2013. p. 373–382.

[12] Segui-Gasco P, Al-Rihani Y, Shin HS, Savvaris A. A novel actuation concept for a multi rotor UAV. J. Intell. Rob. Syst. 2014;74:173–191.

[13] Phang SK, Cai C, Chen BM, et al. Design and mathematical modeling of a 4-standard-propeller (4SP) quadrotor. In: Proceedings of the 10th world congress on intelligent control and automation; 6–8 July 2012; Beijing, China; 2012. p. 3270–3275.

[14] Elfeky M, Elshafei M, Saif AA, et al. Quadrotor helicopter with tilting rotors: modeling and simulation. In: Proceedings of the 2013 world congress on computer and information technology (WCCIT); 2013 Jun 22–24; Sousse, Tunisia; 2013. p. 1–5.

[15] Matsumoto T, Kita K, Suzuki R, et al. A hovering control strategy for a tail-sitter VTOL UAV that increases stability against large disturbance. In: Proceedings of the 2010 IEEE international conference on robotics and automation; 2010 May 3–7; Anchorage (AK); 2010. p. 54–59.